



ASNR Career Center

The Go-To Job Site for Neuroradiology Employers and Job Seekers
Start here: careers.asnr.org

AJNR

T2-weighted three-dimensional turbo spin-echo MR of intracranial aneurysms.

D Rubinstein, E J Sandberg, R E Breeze, S K Sheppard, T G Perkins, A G Cajade-Law and J H Simon

AJNR Am J Neuroradiol 1997, 18 (10) 1939-1943
<http://www.ajnr.org/content/18/10/1939>

This information is current as of December 7, 2023.

T2-Weighted Three-dimensional Turbo Spin-Echo MR of Intracranial Aneurysms

David Rubinstein, Elliot J. Sandberg, Robert E. Breeze, Scott K. Sheppard, Thomas G. Perkins, Ana G. Cajade-Law, and Jack H. Simon

Summary: A T2-weighted three-dimensional turbo spin-echo sequence is described that accurately depicted the anatomy of 18 intracranial aneurysms in 10 patients.

Index terms: Aneurysm, magnetic resonance; Magnetic resonance, technique

T2-weighted three-dimensional turbo spin-echo magnetic resonance (MR) imaging allows examination of the brain with thin sections and a high signal-to-noise ratio (1–3). Because T2-weighted 3-D turbo spin-echo images are characterized by high vascular contrast caused by high signal from surrounding cerebrospinal fluid, moderate signal from adjacent brain, and low signal (black blood) within the vessel, they may be helpful for evaluating intracranial aneurysms. The purpose of this 3-D turbo spin-echo MR imaging study was to compare the depiction of aneurysms by this method against the established method of 3-D time-of-flight MR angiography and with the standard of reference, intraarterial angiography.

Materials and Methods

Ten patients with a total of 18 subarachnoid aneurysms were examined by both intraarterial angiography and T2-weighted 3-D turbo spin-echo MR imaging. Nine of the patients with a total of 12 aneurysms also underwent 3-D time-of-flight MR angiography.

The 3-D turbo spin-echo imaging was performed on a 1.5-T system with the following parameters: 3000/150/1 (repetition time/echo time/excitations), an echo train of 16, 10 3-D slabs, an 18-cm rectangular field of view, and a 177 × 256 matrix. Imaging time was 11 minutes 18

seconds and provided 110 1.5-mm coronal sections with a 0.75-mm overlap (over contiguous acquisition) and 0.7 × 0.7 × 1.5-mm voxels. With these parameters, an antero-posterior dimension of 82 mm was imaged, which covered the most anterior extent of the pericallosal arteries to the origin of the posteroinferior cerebellar arteries. The maximum time between the MR studies and intraarterial angiography was 5 weeks.

For this initial evaluation, the T2-weighted 3-D turbo spin-echo images were compared with intraarterial angiograms and MR angiograms by two nonblinded neuroradiologists. A consensus was reached concerning the 3-D turbo spin-echo studies relative to depiction of the patent lumen of the aneurysms, the parent vessels, and the relationship of the aneurysms to adjacent structures.

Both the 3-D turbo spin-echo and MR angiographic studies were reviewed at a workstation. The 3-D turbo spin-echo sequences were evaluated by scrolling through the original coronal images and multiplanar reformatted (MPR) images. Maximum intensity projections (MIP), source images, and MPR images from the MR angiographic study were used for comparison.

Targeted minimum intensity projections (MINIP) were performed on several of the 3-D turbo spin-echo studies to see if they added useful information, but were not used in the evaluation of the technique.

The imaging findings were compared with the anatomy of six aneurysms (four patients) that were treated surgically.

Results

All 18 aneurysms identified at intraarterial angiography, the standard of reference, were identified on the T2-weighted 3-D turbo spin-echo studies. Sixteen of the 18 aneurysms were identified definitively on the coronal 3-D turbo

Received March 25, 1996; accepted after revision December 13.

Supported in part by Philips Medical Systems, Shelton, Conn.

From the Departments of Radiology (Section of Neuroradiology) (D.R., A.G.C.-L., J.H.S.) and Surgery (Division of Neurosurgery) (R.E.B.), University of Colorado Health Sciences Center, Denver; the Department of Radiology, Denver Veteran's Administration Hospital (E.J.S.); and Philips Medical Systems North America Company, Shelton, Conn (S.K.S., T.G.P.).

Address reprint requests to David Rubinstein, MD, Department of Radiology, Section of Neuroradiology, 4200 E Ninth Ave, Campus Box A-034, Denver, CO 80262.

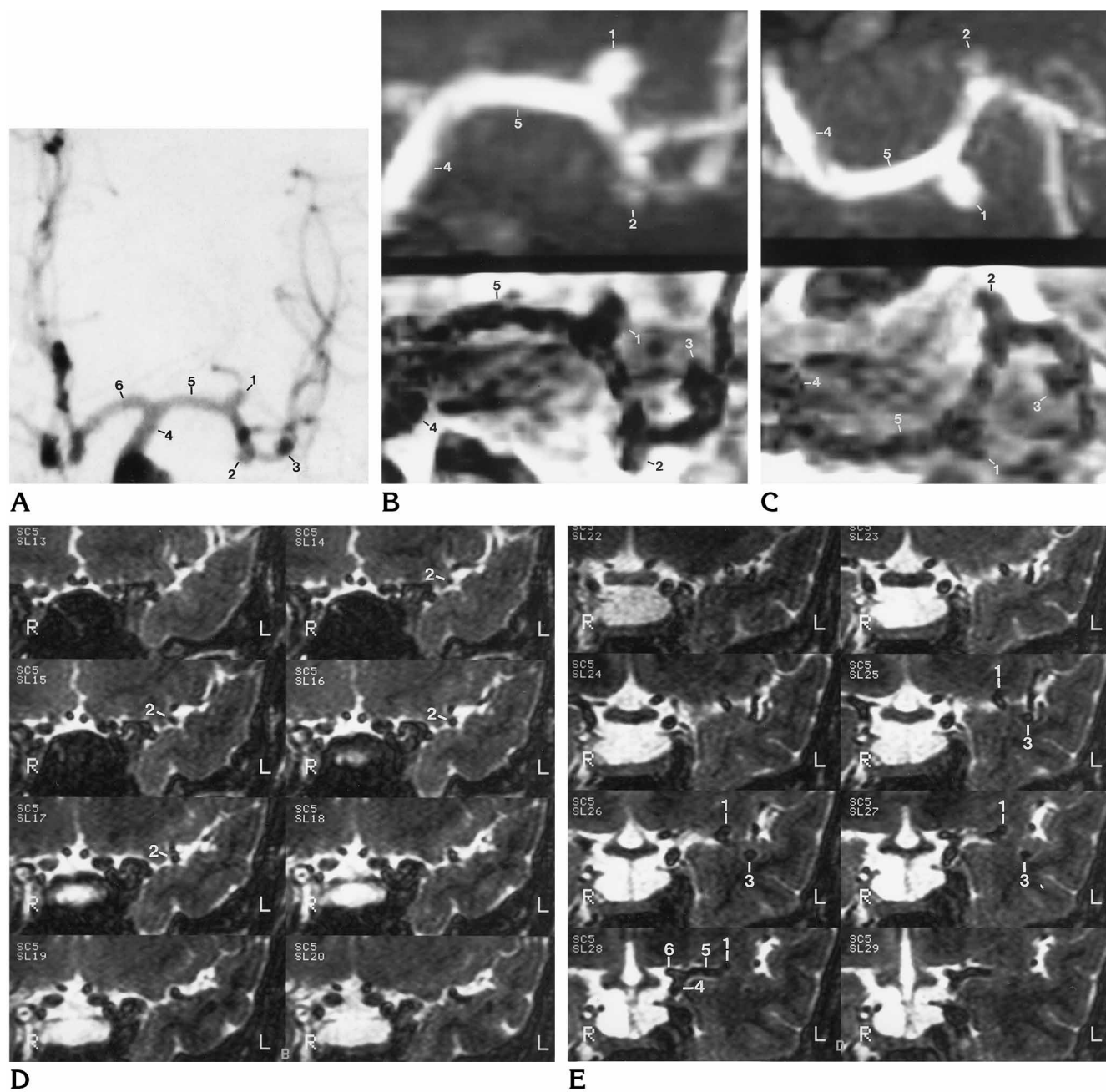


Fig 1. A, Anteroposterior view of left internal carotid angiogram shows three 3-mm aneurysms arising from the proximal left middle cerebral artery.

B, MIP of 3-D time-of-flight MR angiogram targeted to the proximal middle cerebral artery in nearly the same view as the angiogram (top) clearly shows the proximal aneurysm, faintly shows the middle aneurysm, but does not show the distal aneurysm. The MINIP of the T2-weighted 3-D turbo spin-echo image targeted to the same volume (bottom) crudely depicts all three aneurysms.

C, Similarly, the submental vertex view of the time-of-flight MR angiogram (top) shows two of the aneurysms while the MINIP of the turbo spin-echo study (bottom) crudely depicts three aneurysms.

D and E, Sequential 1.5-mm T2-weighted 3-D turbo spin-echo images of the left middle cerebral artery, photographed from anterior to posterior, show three aneurysms. When the left middle cerebral artery and its branches are followed from the most posterior images forward, the small aneurysms appear as branches that end abruptly.

Middle cerebral artery aneurysms (1, 2, 3), left internal carotid artery (4), left middle cerebral artery (5), left anterior cerebral artery (6).

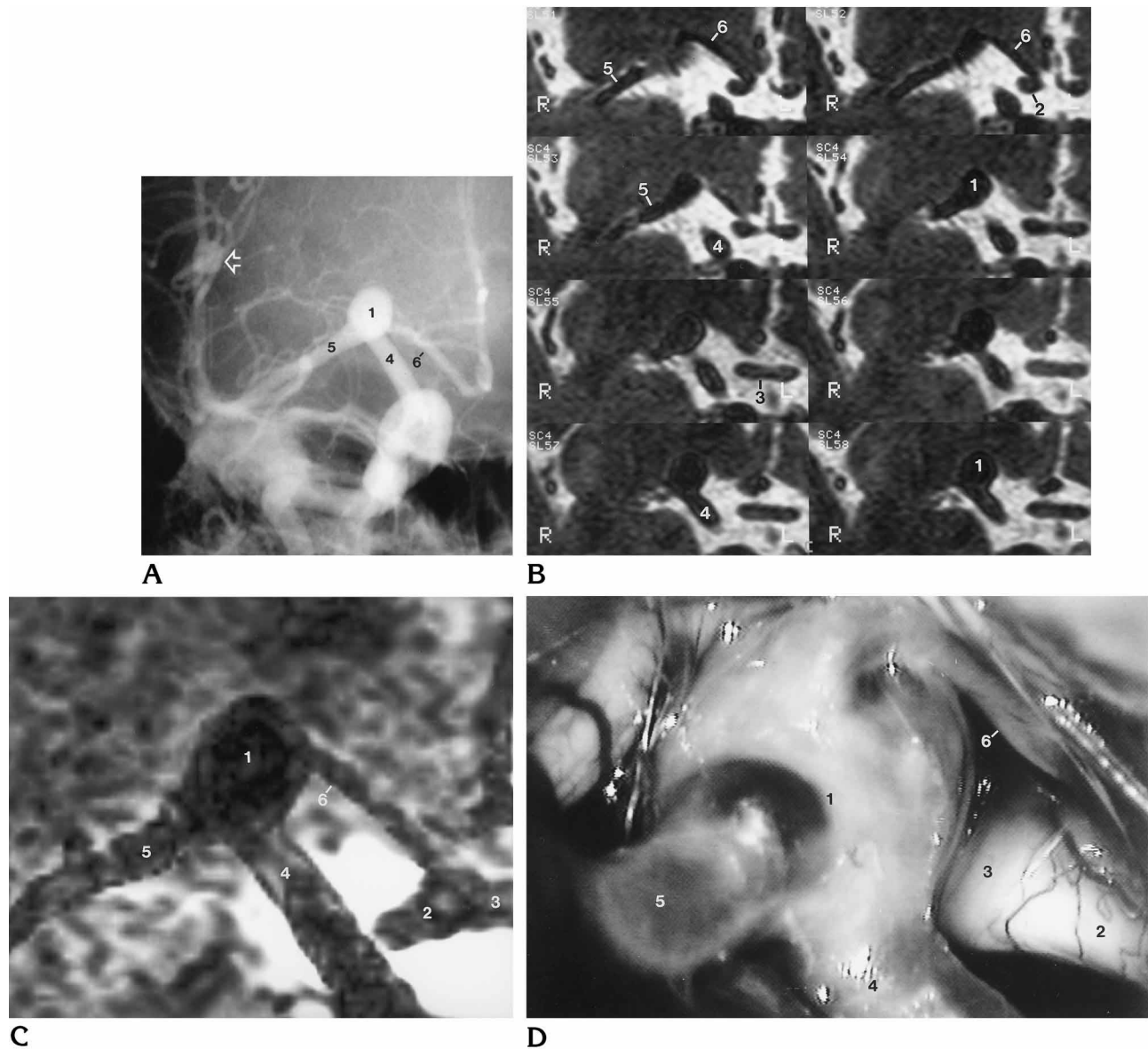


Fig 2. A, Anteroposterior view of right internal carotid arteriogram shows a 6-mm aneurysm at the bifurcation of the right internal carotid artery and a 5-mm aneurysm on a branch of the right middle cerebral artery in the sylvian fissure (arrow).

B, Sequential images from the T2-weighted 3-D turbo spin-echo study, photographed from anterior to posterior, show that the anterior cerebral artery arises from the superior, anterior, and lateral aspects of the carotid aneurysm, a relationship not seen on multiple views of the intraarterial angiogram.

C and D, Targeted MINIP of the 3-D turbo spin-echo data in an anteroposterior view (C) and the surgical photograph taken from a right pterional approach (D) show the same anatomy.

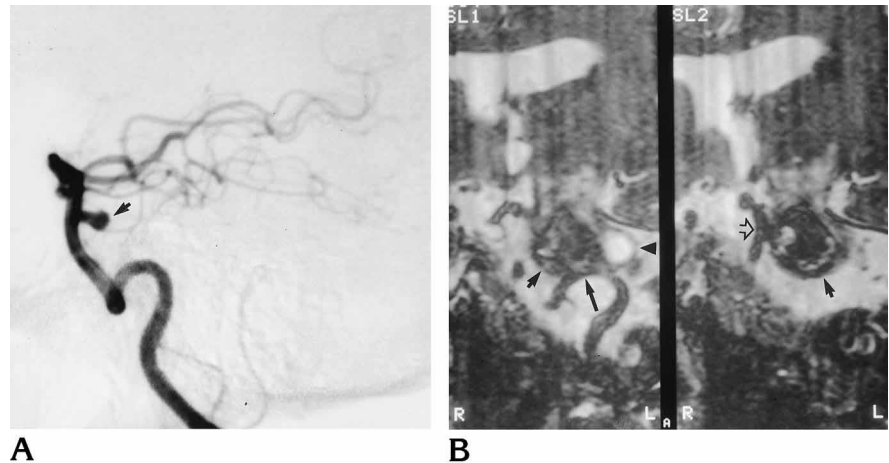
Right internal carotid artery bifurcation aneurysm (1), right optic nerve (2), optic chiasm (3), right internal carotid artery (4), right middle cerebral artery (5), right anterior cerebral artery (6).

spin-echo images (Figs 1 and 2). Two 2-mm aneurysms arising at the origin of the anterior choroidal artery were more clearly depicted on the MPR images along the long axis of the parent vessel or perpendicular to the long axis of the vessel. The original and MPR 3-D turbo spin-echo images showed three aneurysms that were

not visible on either the MIP, MPR, or source images of the time-of-flight MR angiographic studies. One aneurysm was near an aneurysmal clip. A 2-mm aneurysm at the origin of the anterior choroidal artery and a 3-mm aneurysm of the middle cerebral artery were not identified by MR angiography (Fig 1).

Fig 3. A, Lateral view from left vertebral angiogram shows small patent lumen of a distal basilar artery aneurysm (*arrow*).

B, Oblique MPR images from 3-D turbo spin-echo study do not distinguish between the patent lumen and the larger thrombosed portion of the aneurysm (*short solid arrows*). The aneurysm could arise from the basilar artery (*open arrow*) or the left vertebral artery (*long arrow*). A cyst lies in the pons posterior to the aneurysm (*arrowhead*).



The 3-D turbo spin-echo sequence could not differentiate between thrombus and patent lumen in the three partially thrombosed aneurysms. As a result, the site of origin of a mainly thrombosed 18-mm basilar artery aneurysm could not be identified because the thrombosed portion of the aneurysm abutted the left vertebral artery (Fig 3). The 3-D turbo spin-echo original and MPR images, as well as the 3-D time-of-flight MR angiographic source and MPR images, showed the relationship of vessels arising from or adjacent to aneurysms without the confusion presented by overlapping vessels on intraarterial angiography (Fig 2). The 3-D turbo spin-echo sequence was better at depicting the relationship of the aneurysms and surrounding vessels to adjacent structures. The external anatomy seen on 3-D turbo spin-echo images was confirmed at surgery in all four cases (six aneurysms) in which the region of the aneurysm was fully explored.

The MINIP images produced from the entire 3-D turbo spin-echo data set could not depict the aneurysms or vessels because of poor contrast between the vasculature and the brain; however, the MINIP images targeted to a small region surrounding the aneurysms did crudely delineate the aneurysms and the parent vessels (Figs 1 and 2).

Discussion

Our technique of T2-weighted 3-D turbo spin-echo MR imaging has the potential to be more sensitive than 3-D time-of-flight MR angiography in depicting intracranial aneurysms. The original coronal and MPR images of the 3-D

turbo spin-echo sequence showed all the aneurysms. Detection of small aneurysms requires following vessels from section to section so that small aneurysms are not mistaken for branching arteries. This task is most easily performed by scrolling through the image set on a workstation, although even with this technique, small aneurysms arising from the anterior or posterior surfaces of the larger vessels may be difficult or impossible to detect with the original coronal images. MPR images obtained parallel to the long axis of the larger arteries or those that show the arteries in cross-section do depict these aneurysms. Because the MPR images are thin and overlapping, they have nearly the same spatial resolution as the original images do.

The inability to differentiate thrombus from patent lumen (in three aneurysms in our series) is a weakness of the 3-D turbo spin-echo technique, but it does not preclude definition of the external anatomy of the aneurysm and parent vessels and their relationship to adjacent brain.

At present, a disadvantage of the 3-D turbo spin-echo technique is that a 3-D model of the cerebral vasculature cannot be easily produced from the original images. Optimizing scanning parameters to create a greater difference in the signal intensity of the vessels relative to brain may allow easier production of MINIP angiograms in the future. However, MINIP images can be targeted to a small region to help evaluate the aneurysms. In its present state, T2-weighted 3-D turbo spin-echo imaging complements 3-D time-of-flight MR angiography. Further evaluation with prospective blinded methodology is warranted to determine the true sensitivity and

specificity of 3-D turbo spin-echo MR imaging for the detection of intracranial aneurysms.

References

1. Oshio K, Jolesz FA, Melki PS, Mulkern RV. T2-weighted thin-section imaging with the multislab three-dimensional RARE technique. *J Magn Reson Imaging* 1991;1:695-700
2. Yuan C, Schmiedl UP, Weinberger E, Krueck WR, Rand SD. Three-dimensional fast spin-echo imaging: pulse sequence and in vivo image evaluation. *J Magn Reson Imaging* 1993;3:894-899
3. Murakami JW, Weinberger E, Tsurda JS, Mitchell JD, Yuan C. Multislab three-dimensional T2-weighted fast spin-echo imaging of the hippocampus: sequence optimization. *J Magn Reson Imaging* 1995;5:309-315

NOTICE

Beginning January 1, 1998, new manuscripts and correspondence should be sent to the following address:

American Journal of Neuroradiology
2210 Midwest Rd, Suite 207
Oak Brook, IL 60521

Until December 31, 1997, continue to use the current address: Rush-Presbyterian-St Luke's Medical Center, 1653 W Congress Pkwy, Suite KP108, Chicago, IL 60612.